Chapter
3

# Luminescence Analyses (OSL and TL) and AMS Radiocarbon Determinations from Kabazi V

*Rupert A. Housley, David C. W. Sanderson, Chris I. Burbidge, Daniel Richter & Tom F. G. Higham*

Kabazi V was one of a number of Crimean Middle Palaeolithic sites included in the Natural Environment Research Council's EFCHED (Environmental Factors in the Chronology of Human Evolution and Dispersal) initiative (Housley *et al.* 2006). The site was visited in the summer of 2004 and a series of samples was taken for optically-stimulated luminescence (OSL), thermoluminescence (TL) and AMS radiocarbon age determination. Analysis of the samples took place in 2005-2006. This paper reports the findings of these scientific analyses and compares the results with previous analyses that used different geochronology methods.

## Introduction and Sampling

The archaeological, stratigraphic and environmental contexts of this site have been outlined in the publications of Alexander Yevtushenko and in chapters to this monograph by other contributors, and will not be reiterated here (Yevtushenko 1998a, 1998b; Chapters 1, 4, 5, this volume). Based on these previous studies it is clear that the sediments in the buried rock shelter of Kabazi V derive mainly from two principal sources, the hard nummulitic limestone which forms the top of the second ridge cuesta of the Crimean Mountains, and from the weathering of the softer clays and fossiliferous clays that underlie the nummulitic limestone (C. R. Ferring, in Yevtushenko 1998, 274). Several beds of these clays contain abundant nummulitic fossils which were released upon weathering and are contained as clasts within the shelter sediments. It is thus possible that an appreciable proportion of the sedimentation on the site derives from autochthonous sources, from the in situ weathering of the cave roof and walls. However, in determining if optical luminescence dating could be applied successfully to the deposits of the site it is the nature of the allochthonous sediments that is likely to be of more importance, for only if the dated minerals had undergone sufficient exposure to light during transportation will the luminescence signal have been reset to permit successful photo-stimulated dating. Determination of such circumstances was therefore a priority.

Sixteen small OSL profiling samples (in the sense of Burbidge *et al.* 2007) were taken from a vertical profile in 2004. Sampling extended from the base of lithological layer 10 to the upper part of 14B, at c. 10 cm vertical intervals in a column c. 20 from the vertical line separating grid squares 6Б and 6В, such that each stratum was sampled at least once. In all cases, loose material was scraped from the cleaned section into zip lock bags while shaded by a reflective blanket. The purpose of the profiling samples was to survey the suitability of the sediments for a fully quantitative OSL analysis.

Given the many uncertainties that could potentially jeopardize the successful application of OSL in such a sedimentary setting, alternative dating strategies had also to be considered. The need to cross-correlate with other methodologies also determined the need to apply other dating techniques to the site. Although it was realised that the periods of hominin activity at Kabazi V may lie beyond the upper limit of the radiocarbon methodology, it was deemed important to sample for $^{14}C$ especially since $^{14}C$ analyses had not previously been undertaken from the site. A series of six radiocarbon samples was taken from the same cleaned exposed section at Kabazi V as the other samples. These were associated with archaeological levels III/1A, III/1, III/4-5, III/5-3B1 and IV/3. A range of material was selected for dating: burnt bone, bone with or without cut-marks, and charcoal (Table 3-1).

Within the cultural horizons other materials amenable to scientific dating were observed – including heated stones that were possibly suitable for thermoluminescence if of sufficient mass. From the sampled section (grid SW, square 6Б) several lithic clasts, which appeared to have been heated sufficiently, were removed. Unfortunately only two potentially heated clasts of sufficient mass could be found, one of flint and the other of limestone. Both originated from the same archaeological level III/1A (Table 3-2). Despite the poor size of this assemblage the clasts were taken on the understanding they could form a pilot study. Associated field dosimetry readings were made on the surface of the exposed section from where the burnt stones derived in order to help understand the $\gamma$ dosimetry of the site.

Field sampling for quantitative OSL dating was also undertaken on the understanding that the samples could only be dated were the results of the profiling indicated that conditions were right. Quantitative OSL sampling entailed the removal of larger steel tube samples (2 cm diameter, 20 cm length), coupled with a set of environmental dosimetry measurements from the sampling holes. The four large OSL samples came from a vertical section to the left of the profiling positions (section SW, square 6B) and encompassed a series of archaeological levels III/1A, III/4, III/5-3 and IV/1 (Tables 3-2 and 3-4; Fig. 3-1).

Dating was undertaken in separate geochronology laboratories: the OSL profiling and laboratory gamma dosimetry measurements were made in the SUERC at East Kilbride, Scotland; the TL analysis of the heated stones was undertaken in the Department of Human Evolution, Max-Planck-Institute in Leipzig, and AMS $^{14}C$ was made in the Oxford University Radiocarbon Accelerator Unit.

| Sample No. | | Lab No. | Arch. Horizon | Square, Geol. Layer | x | y | z | Material |
|---|---|---|---|---|---|---|---|---|
| EFD4C | 419 | - | III/1A | Sq. 6Б, layer 12 | | | -509 | Cut-marked bone |
| EFD4C | 420 | OxA-X-2134-45 | III/1A | Sq. 6Б, layer 12 | | | -520 to -525 | Burnt bone |
| EFD4C | 421 | - | III/1 | Sq. 6Б, layer 12 | | | -492 | Bone |
| EFD4C | 435 | - | III/4-5 | Sq. 7Б, layer 12 | 3 | 36 | -590 | Bone |
| EFD4C | 436 | OxA-14726 | III/5-3B1 | Sq. 7В, layer 12 | | | | Charcoal |
| EFD4C | 437 | - | IV/3 | Sq. 11Ж | 25 | 35 | -704 | Bone |

**Table 3-1** Accelerator Mass Spectrometry (AMS) $^{14}C$ samples from Kabazi V.

| Sample No. | | Lab No. | Arch. Horizon | Square, Geol. Layer | Sample Type | Depth (cm) |
|---|---|---|---|---|---|---|
| EFD4L | 260 | SUTL 1666 | III/1A | Sq. 6В, layer 12 | OSL tube | -530 |
| EFD4L | 261 | SUTL 1667 | | Sq. 6В, layer 12 | OSL tube | -593 |
| EFD4L | 262 | SUTL 1668 | | Sq. 6В, layer 12A | OSL tube | -625 |
| EFD4L | 263 | SUTL 1669 | | Sq. 6В, layer 14A | OSL tube | -646 |
| EFD4L | 264 | SUTL 1664 | III/1A | Sq. 6Б, layer 12 | TL burnt flint (18.95g) | -522 |
| EFD4L | 265 | SUTL 1665 | III/1A | Sq. 6Б, layer 12 | TL burnt limestone (17.34g) | -519 |
| EFD4L | 276 | SUTL 1663\1 | | Sq. 6Б, layer 10 | Profile black bag | -480 |
| EFD4L | 277 | SUTL 1665\2 | III/1 | Sq. 6Б, layer 12 | Profile black bag | -496 |
| EFD4L | 278 | SUTL 1665\3 | | Sq. 6Б, layer 12 | Profile black bag | -499 |
| EFD4L | 279 | SUTL 1665\4 | | Sq. 6Б, layer 12 | Profile black bag | -515.5 |
| EFD4L | 280 | SUTL 1665\5 | III/1A | Sq. 6Б, layer 12 | Profile black bag | -522.5 |
| EFD4L | 281 | SUTL 1665\6 | | Sq. 6Б, layer 12 | Profile black bag | -529.5 |
| EFD4L | 282 | SUTL 1665\7 | | Sq. 6Б, layer 12 | Profile black bag | -537.5 |
| EFD4L | 283 | SUTL 1665\8 | III/2 | Sq. 6Б, layer 12 | Profile black bag | -543.5 |
| EFD4L | 284 | SUTL 1665\9 | | Sq. 6Б, layer 12 | Profile black bag | -548.5 |
| EFD4L | 285 | SUTL 1665\10 | | Sq. 6Б, layer 12 | Profile black bag | -555.5 |
| EFD4L | 286 | SUTL 1665\11 | | Sq. 6Б, layer 12 | Profile black bag | -566 |
| EFD4L | 287 | SUTL 1665\12 | | Sq. 6Б, layer 12 | Profile black bag | -582 to -587 |
| EFD4L | 288 | SUTL 1665\13 | | Sq. 6Б, layer 12 | Profile black bag | -604 to -608 |
| EFD4L | 289 | SUTL 1665\14 | | Sq. 6Б, layer 12A | Profile black bag | -624 to -627 |
| EFD4L | 290 | SUTL 1665\15 | | Sq. 6Б, layer 14A | Profile black bag | -638 to -643 |
| EFD4L | 291 | SUTL 1665\16 | | Sq. 6Б, layer 14B | Profile black bag | -652 to -656 |

**Table 3-2** Luminescence samples from Kabazi V.

## Luminescence Profiling

### Methodology

A luminescence age is calculated by dividing the radiation dose absorbed by a sample during its burial, by the average dose rate to it during that time, so absorbed dose is a proxy for age. The absorbed dose is actually measured as the laboratory administered dose that produces a signal equivalent to the natural signal, hence the term equivalent dose ($D_e$). The term "luminescence sensitivity" is here used to mean the luminescence signal ($I$) measured per unit absorbed dose ($D$). This is a relative measure, since besides being a product of equipment, set-up, and type of measurement $I$ varies as a function of $D$. The relationship can generally be approximated by a saturating exponential function, which is produced as the traps storing the latent luminescence signal become filled as the sample is exposed to more radiation. In the present study, infrared light (at a mean wavelength of 880 nm), blue light (at 470 nm), and heat were each used to stimulate luminescence signals ($I$) from the samples. Following convention, these signals are termed infrared stimulated luminescence (IRSL), optically stimulated luminescence (OSL), and thermoluminescence (TL) respectively.

Luminescence profiling aims to rapidly produce a stratigraphically detailed survey of a site (Burbidge *et al.* 2007). The objectives are to assess the presence and suitability of particular minerals/grain-sizes/signals for full luminescence dating measurements, and to provide a record of variations in luminescence and related characteristics that can be integrated with archaeological and sedimentological interpretations.

| Sample | | | | Equivalent Dose | | | | | | |
|---|---|---|---|---|---|---|---|---|---|---|
| | | | | Polymineral Fine | | | Polymineral Coarse | | | HFECoarse |
| | Field No | Archaeological | | IRSL | Post-IR OSL | Post-IR&OSL TL | IRSL | Post-IR OSL | Post-IR&OSL TL | OSL |
| SUTL | EFD4L# | Context | Ali | (Gy) | (Gy) | (Gy) | (Gy) | (Gy) | (Gy) | (Gy) |
| 1663 a | 276 | Layer 10 | 1 | 88 ± 23 | 13.2 ± 5.2 | 131 ± 18 | 96.7 ± 3.3 | 96.2 ± 8.0 | 204 ± 4 | ± |
| | | | 2 | 132 ± 32 | 37.6 ± 8.3 | 209 ± 20 | 81.0 ± 1.8 | 77.0 ± 2.9 | 136 ± 2 | ± |
| b | 277 | Layer 12, III/1 | 1 | 137 ± 65 | 38.7 ± 7.6 | 109 ± 11 | 63.3 ± 1.9 | 52.5 ± 2.3 | 109 ± 2 | 74.1 ± 9.9 |
| | | | 2 | 145 ± 45 | 55.1 ± 16.5 | 104 ± 11 | 101 ± 3 | 113 ± 4 | 218 ± 4 | ± |
| c | 278 | Layer 12 | 1 | 90 ± 17 | 37.2 ± 10.1 | 216 ± 39 | 61.4 ± 2.6 | 48.1 ± 3.4 | 92 ± 2 | |
| | | | 2 | 84 ± 18 | 44.3 ± 14.4 | 163 ± 31 | 68.5 ± 2.2 | 96.7 ± 3.8 | 107 ± 2 | ± |
| d | 279 | Layer 12 | 1 | 117 ± 35 | 29.9 ± 5.3 | 131 ± 14 | 69.7 ± 1.7 | 52.6 ± 2.5 | 143 ± 3 | 63.8 ± 4.3 |
| | | | 2 | 109 ± 21 | 3.9 ± 5.7 | 87 ± 7 | 61.4 ± 1.4 | 65.0 ± 2.7 | 167 ± 3 | 41.7 ± 5.6 |
| e | 280 | Layer 12, III/1A | 1 | 68 ± 16 | 32.0 ± 6.3 | 134 ± 15 | 115 ± 3 | 75.5 ± 2.5 | 288 ± 5 | 53.7 ± 4.0 |
| | | | 2 | 95 ± 20 | 24.4 ± 5.0 | 172 ± 26 | 85.0 ± 1.7 | 64.1 ± 1.8 | 190 ± 3 | 61.5 ± 3.5 |
| f | 281 | Layer 12 | 1 | 114 ± 25 | 18.0 ± 5.7 | 93 ± 9 | 70.5 ± 2.1 | 58.0 ± 2.7 | 129 ± 2 | ± |
| | | | 2 | 109 ± 22 | 22.5 ± 9.3 | 70 ± 9 | 64.2 ± 1.2 | 89.3 ± 5.5 | 233 ± 4 | ± |
| g | 282 | Layer 12 | 1 | 141 ± 40 | 22.2 ± 8.5 | 138 ± 19 | 269 ± 11 | 225 ± 18 | 334 ± 7 | ± |
| | | | 2 | 134 ± 49 | 15.4 ± 5.1 | 154 ± 26 | 249 ± 7 | 196 ± 13 | 330 ± 7 | ± |
| h | 283 | Layer 12, III/2 | 1 | 164 ± 23 | 57.5 ± 7.4 | 155 ± 12 | 78.5 ± 3.0 | 68.7 ± 4.6 | 110 ± 2 | 56.1 ± 2.2 |
| | | | 2 | 155 ± 18 | 47.6 ± 7.6 | 139 ± 10 | 82.4 ± 2.1 | 82.3 ± 4.8 | 127 ± 2 | 40.5 ± 1.6 |
| I | 284 | Layer 12, III/3&4 | 1 | | | | 94.7 ± 1.9 | 92.0 ± 2.5 | 145 ± 3 | 33.5 ± 0.9 |
| | | | 2 | | | | 66.3 ± 1.4 | 72.5 ± 2.6 | 139 ± 2 | 48.2 ± 1.3 |
| j | 285 | Layer 12, III/3&4 | 1 | | 72.8 ± 69.0 | | 79.2 ± 1.7 | 91.0 ± 3.1 | 138 ± 2 | 36.9 ± 3.2 |
| | | | 2 | 2 ± 44 | 9.1 ± 28.3 | | 75.7 ± 1.7 | 83.9 ± 2.9 | 181 ± 3 | 41.4 ± 2.5 |
| k | 286 | Layer 12, III/3&4 | 1 | 237 ± 68 | 39.0 ± 7.5 | 113 ± 10 | 49.5 ± 1.4 | 76.8 ± 1.5 | 114 ± 2 | ± |
| | | | 2 | 163 ± 46 | 32.5 ± 4.8 | 133 ± 11 | 66.2 ± 1.4 | 68.2 ± 2.3 | 157 ± 3 | ± |
| l | 287 | Layer 12, III/3&4 | 1 | 140 ± 55 | -7.7 ± -9.4 | 129 ± 20 | 93.6 ± 2.2 | 65.6 ± 2.2 | 161 ± 3 | 143 ± 50 |
| | | | 2 | 127 ± 76 | -6.0 ± -9.7 | 251 ± 110 | 74.5 ± 1.5 | 73.8 ± 2.9 | 141 ± 2 | 60.3 ± 5.1 |
| m | 288 | Layer 12, III/3&4 | 1 | 64 ± 15 | 43.7 ± 8.6 | 113 ± 13 | 67.8 ± 2.2 | 42.0 ± 1.9 | 135 ± 3 | ± |
| | | | 2 | 37 ± 19 | 70.9 ± 25.1 | 900 ± 1339 | 105 ± 3 | 87.3 ± 4.3 | 118 ± 2 | ± |
| n | 289 | Layer 12A, III/5 | 1 | 51 ± 17 | 52.3 ± 20.7 | 284 ± 93 | 78.5 ± 1.6 | 94.1 ± 3.7 | 248 ± 4 | ± |
| | | | 2 | 74 ± 30 | 13.2 ± 13.0 | | 57.4 ± 1.7 | 43.9 ± 2.0 | 90 ± 2 | ± |
| o | 290 | Layer 14A, IV/4 | 1 | 3 ± 11 | | | 196 ± 4 | 188 ± 9 | 359 ± 7 | 53.1 ± 9.2 |
| | | | 2 | | | 459 ± 238 | 147 ± 3 | 208 ± 7 | 298 ± 5 | |
| p | 291 | Layer 14B, V | 1 | 241 ± 50 | 68.5 ± 22.1 | 386 ± 44 | 240 ± 5 | 304 ± 9 | 459 ± 8 | 80.4 ± 9.7 |
| | | | 2 | 333 ± 187 | 31.1 ± 9.2 | 417 ± 59 | 173 ± 3 | 178 ± 7 | 360 ± 6 | 53.4 ± 4.0 |

**Table 3-3a** Equivalent dose estimates for polymineral, polymineral coarse, and etched (quartz) fractions from Kabazi V, in Grays (Gy).

Preparation of the profiling samples produced three separate mineral/grain-size fractions that would be analysed for a number of properties:

1. Polymineral sand-sized fraction ("polymineral coarse", PMC)
2. Quartz enriched sand sized fraction ("hydrofluoric-etched coarse", HFC)
3. Polymineral silt-sized fraction ("polymineral fine", PMF)

To produce these fractions preparatory treatments were applied to approximately 5 g of bulk sample (for details of the procedures see Fig. 3-2). The samples were initially wet sieved, to reduce the chance of contamination by geological grains from limestone clasts. Carbonates were then removed from the 90-250 μm fraction using HCl acid, and after thorough rinsing in water to clean the grains, sufficient of the polymineral coarse material was

| Sample | | | | Sensitivity | | | | | | |
|---|---|---|---|---|---|---|---|---|---|---|
| | | | | Polymineral Fine | | | Polymineral Coarse | | | HFE Coarse |
| | Field No | Archaeological | | IRSL | Post-IR OSL | Post-IR&OSL TL | IRSL | Post-IR OSL | Post-IR&OSL TL | OSL |
| SUTL | EFD4L# | Context | Ali | (cps/Gy) | (cps/Gy) | (cp°C/Gy) | (cps/Gy) | (cps/Gy) | (cp°C/Gy) | (cps/Gy) |
| 1663 a | 276 | Layer 10 | 1 | 0.46 ± 0.10 | 1.81 ± 0.21 | 0.14 ± 0.02 | 10.1 ± 0.3 | 5.4 ± 0.4 | 6.0 ± 0.1 | 0.4 ± 0.1 |
| | | | 2 | 0.46 ± 0.10 | 1.53 ± 0.22 | 0.21 ± 0.02 | 46.8 ± 0.9 | 28.0 ± 0.9 | 21.7 ± 0.4 | ± |
| b | 277 | Layer 12, III/1 | 1 | 0.22 ± 0.10 | 1.61 ± 0.20 | 0.21 ± 0.02 | 17.3 ± 0.4 | 19.4 ± 0.6 | 8.1 ± 0.1 | 9.5 ± 0.3 |
| | | | 2 | 0.36 ± 0.10 | 0.84 ± 0.19 | 0.20 ± 0.02 | 25.0 ± 0.6 | 18.7 ± 0.6 | 5.9 ± 0.1 | ± |
| c | 278 | Layer 12 | 1 | 0.69 ± 0.11 | 1.19 ± 0.19 | 0.11 ± 0.02 | 7.5 ± 0.3 | 7.5 ± 0.4 | 3.3 ± 0.1 | 7.0 ± 0.2 |
| | | | 2 | 0.56 ± 0.10 | 0.86 ± 0.19 | 0.09 ± 0.02 | 13.7 ± 0.4 | 16.3 ± 0.5 | 6.9 ± 0.1 | ± |
| d | 279 | Layer 12 | 1 | 0.41 ± 0.11 | 2.27 ± 0.22 | 0.19 ± 0.02 | 30.3 ± 0.7 | 18.1 ± 0.6 | 9.9 ± 0.2 | 21.9 ± 0.5 |
| | | | 2 | 0.65 ± 0.11 | 1.50 ± 0.21 | 0.30 ± 0.02 | 41.2 ± 0.8 | 24.0 ± 0.8 | 16.0 ± 0.3 | 11.7 ± 0.3 |
| e | 280 | Layer 12, III/1A | 1 | 0.57 ± 0.10 | 1.85 ± 0.21 | 0.18 ± 0.02 | 32.8 ± 0.7 | 32.6 ± 0.9 | 14.7 ± 0.3 | 20.3 ± 0.5 |
| | | | 2 | 0.61 ± 0.11 | 2.24 ± 0.23 | 0.13 ± 0.02 | 77.8 ± 1.5 | 54.8 ± 1.3 | 21.9 ± 0.4 | 36.0 ± 0.7 |
| f | 281 | Layer 12 | 1 | 0.55 ± 0.11 | 1.71 ± 0.21 | 0.22 ± 0.02 | 17.1 ± 0.4 | 16.8 ± 0.6 | 7.3 ± 0.1 | ± |
| | | | 2 | 0.60 ± 0.11 | 1.03 ± 0.20 | 0.19 ± 0.02 | 105 ± 1.9 | 12.5 ± 0.6 | 18.8 ± 0.3 | ± |
| g | 282 | Layer 12 | 1 | 0.40 ± 0.11 | 1.14 ± 0.18 | 0.13 ± 0.02 | 5.6 ± 0.2 | 4.8 ± 0.3 | 4.1 ± 0.1 | ± |
| | | | 2 | 0.30 ± 0.10 | 1.85 ± 0.20 | 0.11 ± 0.02 | 10.8 ± 0.3 | 6.0 ± 0.4 | 4.8 ± 0.1 | ± |
| h | 283 | Layer 12, III/2 | 1 | 0.91 ± 0.12 | 2.32 ± 0.23 | 0.29 ± 0.02 | 8.5 ± 0.3 | 7.4 ± 0.4 | 3.3 ± 0.1 | 107 ± 2.0 |
| | | | 2 | 1.12 ± 0.12 | 2.02 ± 0.22 | 0.32 ± 0.02 | 22.1 ± 0.5 | 9.9 ± 0.5 | 8.2 ± 0.2 | 98.7 ± 1.8 |
| I | 284 | Layer 12, III/3&4 | 1 | 0.09 ± 0.09 | 0.56 ± 0.18 | -0.02 ± -0.02 | 68.3 ± 1.3 | 51.3 ± 1.2 | 22.1 ± 0.4 | 277 ± 4.8 |
| | | | 2 | 0.01 ± 0.09 | 0.59 ± 0.17 | 0.00 ± -0.02 | 61.6 ± 1.2 | 31.6 ± 0.9 | 20.0 ± 0.3 | 298 ± 5.2 |
| j | 285 | Layer 12, III/3&4 | 1 | -0.03 ± -0.10 | 0.21 ± 0.16 | 0.02 ± 0.02 | 50.4 ± 1.0 | 30.1 ± 0.9 | 15.6 ± 0.3 | 21.9 ± 0.5 |
| | | | 2 | -0.10 ± -0.09 | 0.29 ± 0.17 | 0.02 ± 0.02 | 45.0 ± 0.9 | 28.0 ± 0.8 | 12.9 ± 0.2 | 38.4 ± 0.8 |
| k | 286 | Layer 12, III/3&4 | 1 | 0.42 ± 0.12 | 1.74 ± 0.21 | 0.24 ± 0.02 | 22.7 ± 0.5 | 170 ± 3.1 | 10.6 ± 0.2 | ± |
| | | | 2 | 0.43 ± 0.11 | 2.72 ± 0.24 | 0.24 ± 0.02 | 61.2 ± 1.2 | 37.7 ± 1.0 | 16.7 ± 0.3 | ± |
| l | 287 | Layer 12, III/3&4 | 1 | 0.28 ± 0.10 | 0.90 ± 0.19 | 0.12 ± 0.02 | 34.5 ± 0.7 | 34.1 ± 0.9 | 14.9 ± 0.3 | 5.6 ± 0.2 |
| | | | 2 | 0.17 ± 0.10 | 0.76 ± 0.18 | 0.04 ± 0.02 | 73.2 ± 1.4 | 25.3 ± 0.8 | 19.6 ± 0.3 | 19.8 ± 0.5 |
| m | 288 | Layer 12, III/3&4 | 1 | 0.56 ± 0.10 | 1.50 ± 0.20 | 0.18 ± 0.02 | 13.2 ± 0.4 | 19.2 ± 0.6 | 5.0 ± 0.1 | ± |
| | | | 2 | 0.32 ± 0.10 | 0.62 ± 0.18 | 0.01 ± 0.02 | 22.9 ± 0.5 | 13.7 ± 0.6 | 7.4 ± 0.1 | ± |
| n | 289 | Layer 12A, III/5 | 1 | 0.43 ± 0.10 | 0.63 ± 0.19 | 0.06 ± 0.02 | 55.9 ± 1.1 | 26.4 ± 0.8 | 19.2 ± 0.3 | ± |
| | | | 2 | 0.29 ± 0.10 | 0.63 ± 0.17 | -0.03 ± -0.02 | 18.7 ± 0.5 | 19.1 ± 0.6 | 8.5 ± 0.2 | ± |
| o | 290 | Layer 14A, IV/4 | 1 | 0.40 ± 0.10 | 1.17 ± 0.18 | -0.05 ± -0.02 | 28.2 ± 0.6 | 11.4 ± 0.5 | 9.6 ± 0.2 | 5.7 ± 0.2 |
| | | | 2 | -0.09 ± -0.09 | 0.04 ± 0.17 | 0.03 ± 0.02 | 34.1 ± 0.7 | 33.1 ± 1.0 | 40.7 ± 0.7 | 4.2 ± 0.2 |
| p | 291 | Layer 14B, V | 1 | 0.51 ± 0.10 | 0.75 ± 0.19 | 0.16 ± 0.02 | 66.7 ± 1.3 | 33.6 ± 1.0 | 20.9 ± 0.4 | 14.1 ± 0.4 |
| | | | 2 | 0.18 ± 0.10 | 1.26 ± 0.19 | 0.12 ± 0.02 | 51.6 ± 1.0 | 21.6 ± 0.7 | 17.2 ± 0.3 | 28.5 ± 0.6 |

**Table 3-3b** Luminescence sensitivities, in photon counts per second per Gray from polymineral and etched quartz fractions from Kabazi V.

removed to make up three aliquots. The remaining material was HF etched to produce a quartz-rich fraction. The less than 90 μm fraction was settled in water for 2 mins and the suspended (less can c. 20 μm) fraction collected and centrifuged out for further processing. Approximately 2 ml of this was treated in $H_2O_2$ and HCl acid to remove organics and carbonates, and the undissolved material settled in acetone to isolate the 4-11 μm fraction, which was itself settled onto steel discs in acetone.

Two aliquots from each fraction were subjected to simple regenerative $D_e$ determinations, using IRSL, post-IR OSL, and post-IR&OSL TL for the polymineral fractions, and sensitivity corrected OSL for the HF etched fraction. This rapidly produced large matrices of luminescence sensitivity and $D_e$ values from top to base of the section, including paired reproducibility assessment.

## Results

The results, plotted in stratigraphic order, are shown in Figs. 3-3a and 3-3b, together with a column showing the results of the field gamma spectrometry which indicate changes in dose rate down the section. The individual sample determinations are summarised in Tables 3-3a and 3-3b.

Little quartz was obtained from many of the samples, but what was recovered had similar, if variable, sensitivity to the polymineral coarse fraction. The fines were less sensitive for all signals. It is notable that the ashy level (III/1A) had similar sensitivity to sterile sediments above and below it. This indicates that the materials used for profiling were little affected by any heating.

The polymineral coarse fraction yielded the most consistent patterns in $D_e$: similar values were obtained through the section, except for the bottom (lithological layers 14A and 14B) and a single sample from just above archaeological context III/2 in lithological layer 12. IRSL and post-IR OSL gave values of c. 60-80 Gy for most samples, and c. 150-250 Gy for the exceptions. Post-IR&OSL TL values were around 1.5 times these, and increased scatter was evident in the upper section. Post-IR&OSL TL on the polymineral fine fraction yielded similar patterns and values to post-IR&OSL TL on the polymineral coarse fraction. However, $D_e$ values from IRSL on the polymineral fine fraction varied from c. 50 to 150 Gy through most of the section, exhibiting variable results (c. 80-140 Gy) above archaeological context III/1A, a steady rise (c. 70-155 Gy) between III/1A and III/2, a decline to c. 50 Gy in lithological layer 12A, and then much higher values in layer 14. In the upper half of the section, post-IR OSL from the fines approximately mirrored the pattern of IRSL results but with much lower values (c. 15 – 40 Gy). Lower in the section post-IR OSL results were highly scattered. OSL measurements on the HF etched coarse fraction exhibit a decrease through the upper half of the section, from c. 70 Gy to c. 40 Gy. Results from below this are more scattered, but comparison of the $D_e$ values of 50-80 Gy obtained from the lowermost layers with those from the polymineral fractions, indicates both that the HFC results may be strongly affected by saturation of the signal from quartz, and that the IRSL and post-IR OSL signals from the PMC fraction came from similar (non quartz) minerals.

Using alpha, beta and gamma dose rates calculated from full series parent radionuclide concentrations estimated by laboratory gamma spectrometry (Table 3-3a, 3-5), with correction for *in-situ* water content and the addition of an approximate cosmic ray dose rate of 0.15 mGy/a, many of the fractions and

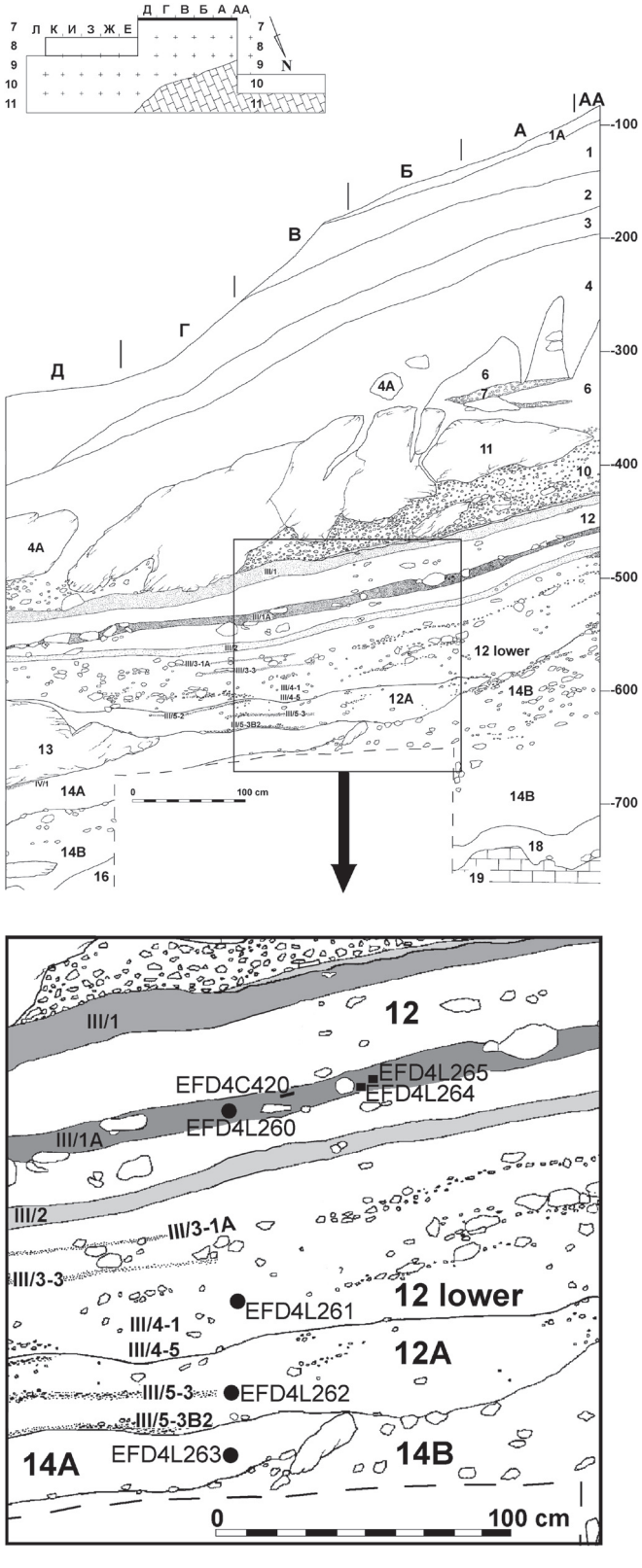


**Fig. 3-1** Section at Kabazi V in 2004 showing position of OSL and TL samples in squares 6В and 6Б.

| **Kabazi V** | **Field Gamma dosimetry results** | | | | | |
|---|---|---|---|---|---|---|
| Reference | Geometry (pi) | Measured dose rate /mGy a-1 | | Geometrically corrected dose rate /mGy/a | | |
| EFD4G080 | 3.8 | 0.17 | ±0.01 | | | Exploratory surface of section |
| EFD4G088 | 4 | 0.20 | ±0.01 | 0.20 | ±0.02 | Hole associated with EFD4L260 |
| EFD4G089 | 4 | 0.19 | ±0.01 | 0.19 | ±0.02 | Hole associated with EFD4L261 |
| EFD4G090 | 4 | 0.18 | ±0.01 | 0.18 | ±0.02 | Hole associated with EFD4L262 |
| EFD4G091 | 4 | 0.20 | ±0.01 | 0.20 | ±0.02 | Hole associated with EFD4L263 |
| EFD4G092 | 3.8 | 0.18 | ±0.01 | 0.20 | ±0.02 | Surface layer III/1A |
| EFD4G093 | 3.8 | 0.17 | ±0.01 | 0.20 | ±0.02 | Surface burnt flint EFD4L264 |
| EFD4G094 | 3.8 | 0.18 | ±0.01 | 0.20 | ±0.02 | Surface associated with EFD4L265 |
| | | | | | | |
| Mean | | 0.184 | | 0.196 | | |
| Std Dev | | 0.012 | | 0.008 | | |
| Std Err | | 0.004 | | 0.003 | | |

**Table 3-4** Field gamma dosimetry results from Kabazi V.

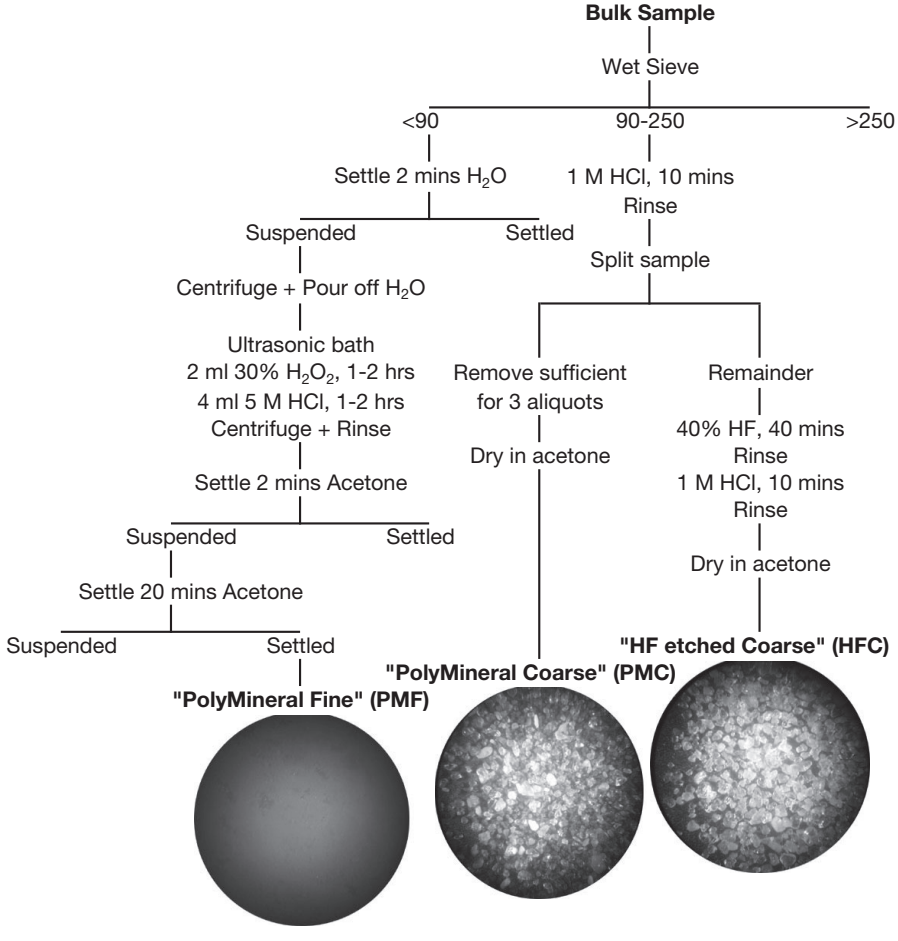


**Fig. 3-2** Preparation of "polymineral fine", "polymineral coarse" and "hydrofluoric etched coarse" mineral/grain-size fractions from profiling samples.

signals indicate apparent ages in the range c. 60-100 ka for the majority of the section, and c. 200 ka for layer 14.

The results of luminescence profiling at Kabazi V present a dilemma, particularly with respect to data from the polymineral coarse fraction. High $D_e$ values at the base and in one sample from the middle of the section indicate that the relatively consistent lower values from the majority of samples are not strongly affected by the inclusion of older (geological) material and/or residual signals. Limestone clast samples from the same geological formation were taken at Kabazi II. These yielded similar or higher $D_e$ values than those from the base of the Kabazi V section. This implies that the OSL signals in the coarse grains of most samples from Kabazi V were reset in the 60-100 ka range of apparent ages. However, this is substantially older than most of the independent dating evidence. Also, the geomorphological context of these samples and their lack of progression in $D_e$ with depth (until the base of the section) are consistent with the accumulation of material with residual luminescence age.

In summary then, profiling indicates that either OSL signals were bleached at deposition and layer 12 accumulated circa OIS 4, or that OSL signals were bleached c. OIS 4 and layer 12 accumulated later by reworking of this material without substantial light or heat exposure.

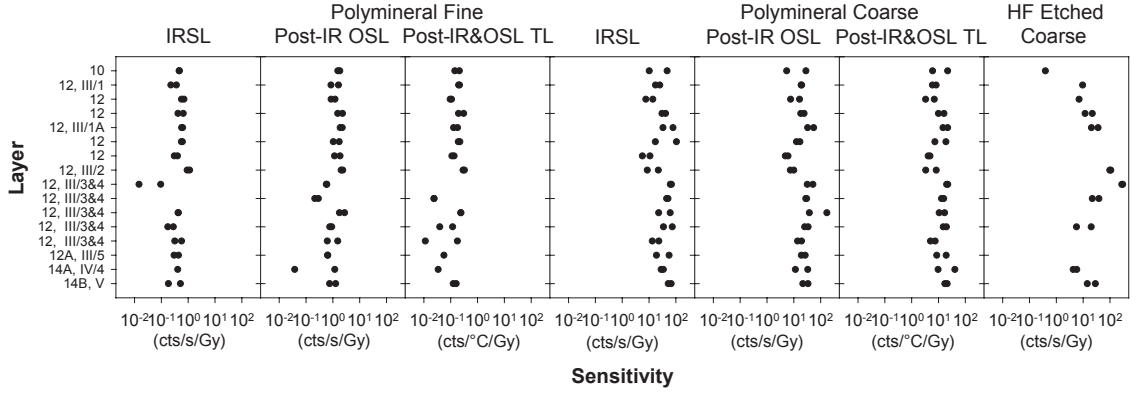


**Fig. 3-3a** Luminescence profiling results from Kabazi V, showing the sensitivity of the samples to luminescence (from Burbidge *et al.*, 2005, Fig. 5.5). Samples are plotted in stratigraphic order.

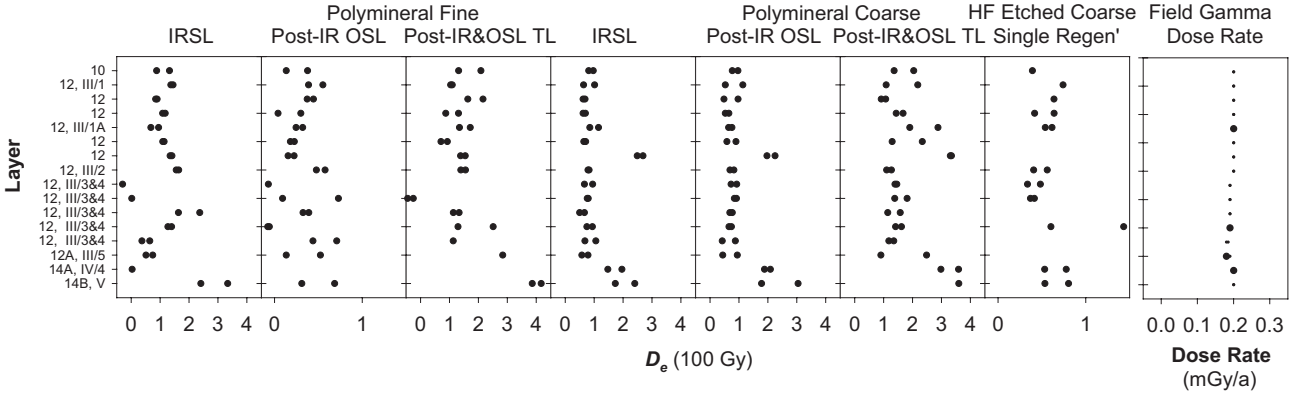


**Fig. 3-3b** Luminescence profiling results from Kabazi V, with field dosimetry results (from Burbidge *et al.*, 2005, Fig. 5.5). Samples are plotted in stratigraphic order. Note changes in $D_e$ scale with mineral/grain size fraction. Smaller points in the plot of field gamma dose rate are interpolated values.

| Sample | Potassium (%) | | Thorium (ppm) | | Uranium apparent concentration (ppm) | | | | | | | | |
|---|---|---|---|---|---|---|---|---|---|---|---|---|---|
| | | | Full series | | Full series | | Pre-Radon | | Post Radon | | From $^{210}$Pb | | Water content (%) |
| SUTL1666 | 0.230 | ±0.02 | 1.622 | ±0.10 | 1.736 | ±0.08 | 3.723 | ±1.374 | 1.610 | ±0.09 | 1.13 | ±0.61 | 0.060 |
| SUTL1667 | 0.230 | ±0.02 | 1.550 | ±0.05 | 1.682 | ±0.05 | 2.252 | ±0.650 | 1.632 | ±0.06 | 1.25 | ±0.44 | 0.050 |
| SUTL1668 | 0.200 | ±0.02 | 1.584 | ±0.10 | 1.636 | ±0.08 | 1.742 | ±1.090 | 1.627 | ±0.11 | 1.30 | ±0.60 | 0.070 |
| SUTL1669 | 0.320 | ±0.02 | 2.015 | ±0.06 | 1.672 | ±0.05 | 1.375 | ±0.580 | 1.703 | ±0.06 | 1.89 | ±0.44 | 0.100 |
| | | | | | | | | | | | | | |
| Mean | 0.245 | | 1.692 | | 1.682 | | 2.273 | | 1.643 | | 1.39 | | 0.070 |
| Std Dev | 0.051 | | 0.216 | | 0.041 | | 1.03 | | 0.041 | | 0.34 | | 0.024 |

**Table 3-5** High resolution gamma spectrometry results from bulk samples associated with OSL sampling tubes.

## Field dosimetry measurements

Gamma dose rates were recorded on site using a 2x2″ NaI scintillation probe and portable gamma spectrometer (Health Physics Instruments Rainbow MCA). Spectra were collected for 600s periods from eight measurement locations and were converted to dose rates using standard SUERC procedures. The instrument had been checked and calibrated using the doped concrete calibration pads at SUERC before commencement of fieldwork in July 2004, and was rechecked in September 2004 on conclusion of the fieldwork. Dose rates were estimated using three conversion methods (integral count rates > 450 keV, integral count rates >1350 keV and an energy integration method) and corrected for field geometry. The results are tabulated in Table 3-4. Readings EFD4G 088-91 were recorded in $4\pi$ geometry in the sample holes used to collect tube samples for possible luminescence dating; a further 4 observations were made with the detector presented to the face of the excavated stratigraphy, estimated to be in $3.8\pi$ geometry. Of these readings EFD4G 093 is in the position of the burnt flint sample EFD4L 264 which has been subjected to TL measurements at the Leipzig Max Planck Institute for Evolutionary Anthropology. From Table 3-4 it can be seen that the gamma ray does rates inferred from in-situ measurements are highly consistent from position to position, with a mean value of 0.196±0.008 mGy $a^{-1}$. The instrument calibration is believed to be accurate with a systematic uncertainty of approximately 10%, which should be taken into account in age estimation based on these data.

## Laboratory gamma spectrometry

Bulk samples of sediments associated with OSL tube sampling were dried, ground, and analysed by high resolution gamma spectrometry at SUERC. From Kabazi V the four OSL tube sampling positions have been examined in this manner. Samples were sealed for >3 weeks after drying and grinding to allow Radon daughters to equilibriate, and then measured for periods of 25-100 ks in a shielded Ortec GMX detector of 50% relative efficiency. Gamma ray lines associated with $^{40}$K and nuclides from the $^{238}$U and $^{232}$Th decay series were quantified and used to estimate radionuclide concentrations, scaled relative to an internal Shap Granite standard presented in similar form. Table 3-5 summarises the radionuclide parent concentrations. For the $^{40}$K this was based on the gamma emission at 1462 keV; for the Th decay series on the weighted mean results from lines from $^{228}$Ac, $^{212}$Pb, $^{212}$Bi, and $^{208}$Tl; and for the U decay series on analysis of lines from $^{234}$Th, $^{226}$Ra (and $^{235}$U), $^{214}$Bi, $^{214}$Pb, and $^{210}$Pb. Results in Table 3-5 from the Th decay series are expressed as Th elemental concentrations based on full-series radioactive equilibrium. The K and Th concentrations are broadly consistent between samples, with slightly elevated concentrations in the bottom sample of the sequence (SUTL1669), and mean values of 0.245±0.05 % K and 1.69±0.22 ppm Th respectively. For the Uranium series apparent parent concentrations are also tabulated inferred from (i) the full series weighted according to the relative gamma ray emission intensities of all nuclides analysed, (ii) the pre-radon nuclides (lines from $^{234}$Th and $^{226}$Ra), (iii) post-radon nuclides ($^{214}$Bi and $^{214}$Pb) and (iv) $^{210}$Pb. The full series and post-Rn estimates are closely aligned (reflecting the dominant influences on precision obtained from the high intensity emissions from post-Rn U

series nuclides) with mean apparent concentrations of 1.68 and 1.64 ppm respectively. Estimated concentrations from the pre-radon nuclides show slightly higher values in the top two samples, which may reflect recent dissolved uranium deposition within the last few thousands years, in the limestone system of the site. Uranium concentrations based on $^{210}$Pb are slightly lower with a mean value of 1.39 ppm and show increasing concentrations with depth, which are attributed to a greater probability of radon loss through diffusion to the surface in the upper layers compared with deeper samples.

Table 3-6 shows the gamma dose rate contributions from K, Th and U series based on the mean results of all samples, and taking the diverse U series apparent concentrations tabulated above. Also shown are total dose rate estimates from the full series, post radon and $^{210}$Pb scenarios, both for the dry sample and for samples in wet condition, based on the weight losses recorded during sample drying. Dose rate conversions factors were based on those of Aitken (1983) and the water content correction formula of Aitken (1985).

Since the gamma spectrometry samples had been sealed prior to counting, thus avoiding radon loss under laboratory conditions, it is to be expected that full series estimates of the wet dose rates would be higher in general than gamma dose rates observed in the field. This is indeed so, with the mean value of 0.315 ± 0.018 being significantly greater than the field recorded value of 0.196 ± 0.008 mGy a$^{-1}$; however the difference between these estimates cannot be reconciled by radon loss alone. The predicted gamma dose rates based on the $^{210}$Pb derived uranium estimates, which are arguably the most appropriate means of estimating average radon retention under field conditions, would lead to predicted gamma dose rates of 0.284 ± 0.04 mGy a$^{-1}$; again in excess of the observed field values. Noting that radon loss is greater for the upper samples than deeper layers, the total gamma dose rate predicted for the depth of sample SUTL1666 (corresponding to the same layer as the flint samples) is 0.258 ± 0.07 mGy a$^{-1}$; this is in slightly better agreement with the gamma results. However, the general pattern of observation is that the laboratory gamma analyses are associated with higher dose rate estimates than field observations by some 20 % or more even after consideration of water content and radon loss in the field. Given that the spatial response of the field measurements extends to 10-30 cm from the measurement position, and will include limestone clasts of all sizes present, whereas the laboratory sample originates from within approximately 5-10 cm of the sampling tube position and will have excluded the larger limestone clasts present on site, it is argued that the data imply an enhanced concentration of radionuclides in the finer fractions represented to a greater extent within the laboratory sample than the field observations.

On this basis the mean field dose rates are preferred as basis of estimates of the gamma dose rates to burnt flints and sediment samples undergoing luminescence dating. The laboratory gamma results provide additional information on the concentration variations with position on a finer scale than possible with the field instrument, and also give information about the recent movement of uranium in the upper layers sampled, plus the general state of radon retention under recent field conditions.

| **Sample** | **Potassium** | | **Thorium** | | **Uranium** | | | | | | | |
|---|---|---|---|---|---|---|---|---|---|---|---|---|
| | | | Full series | | Full series | | Pre-Radon | | Post Radon | | From $^{210}$Pb | |
| Dry Gamma dose rate /mGy a$^{-1}$ | 0.059 | ±0.013 | 0.087 | ±0.011 | 0.193 | ±0.005 | 0.261 | ±0.119 | 0.189 | ±0.005 | 0.160 | ±0.039 |
| | | | | | | | | | | | | |
| Total Gamma dose rate /mGy a$^{-1}$ | | | | | 0.339 | ±0.017 | | | 0.335 | ±0.017 | 0.306 | ±0.042 |
| | | | | | | | | | | | | |
| Wet Gamma dose rate /mGy a$^{-1}$ | | | | | 0.315 | ±0.018 | | | 0.311 | ±0.018 | 0.284 | ±0.040 |

**Table 3-6** Gamma dose rate estimates for dry samples and wet matrices.

# Thermoluminescence

## Sampling

Two heated rock samples from a single layer at Kabazi V were submitted to the luminescence dating laboratory at the Department of Human Evolution at the Max-Planck-Institute for Evolutionary Anthropology, Leipzig, Germany for dating with thermoluminescent methods (Table 3-2). The macroscopic features that suggest an alteration of the samples by fire were the presence of surface cracking and 'potlid' structures (in sample EFD4L 264), and a grey surface colour (in EFD4L 265).

Sample EFD4L 265 was a limestone fragment that appears to have been heated. Currently there is no established preparation method for dating such material since the few studies which have investigated the TL dating potential of such samples (e.g. Roque et al., 2001) have reported ambiguous results. For this reason no further work was undertaken on this sample.

## Sample preparation

Sample EFD4L 264 was prepared for TL-dating by stripping off the outer 2 mm layer with a low speed water cooled diamond saw. This removes parts which might have been bleached and all parts of the sample which had been exposed to $\alpha$ and $\beta$-radiation from the surrounding sediment. These radiations thus can be excluded from the age calculation, which improves the precision of the resulting ages. The remaining material was gently crushed in a hydraulic steel mortar. About 200 mg of powder were used for measurements of radioactive element concentrations by ICP-MS (Inductively-Coupled-Plasma Mass-Spectrometry) and INAA (Instrumental Neutron Activation Analysis). The grain fraction of 90-160 μm for the determination of the palaeodose was then obtained by sieving, while the fine grain of 4-11 μm material for alpha sensitivity measurements was prepared after Zimmermann (1971).

## Testing for sufficiency of heating for TL-dating

In general prehistoric heating temperatures in excess of about 400°C (Melcher & Zimmerman 1977) are necessary for a successful application of the TL-dating method to heated flint samples. To ascertain that this had happened, a small sub-sample was removed from the edges of the clast. Crushed, sieved and treated with HCl the resulting grains were mounted on a set of four discs to test for the sufficiency of heating for TL analysis before the entire sample was subjected to the rather time consuming (and destructive) full dating procedure. Two of the sets of four discs received a β-dose and the resulting TL glow curve of all the discs from the one sample is shown in Fig. 3-4.

For TL dating only signals above approximately 300°C are of interest. This is because the stability of the signal below this temperature is not sufficiently good to be applied to samples from this time period. Sample EFD4L 264 showed a natural TL peak (NTL in blue) at around 360 °C. Additional β-irradiation increases the TL signal proportionally over the temperature range of the peak, thus providing a heating plateau (ratio of NTL+β/NTL) over the TL-peak (Fig. 3-5). This feature shows that the sample had undergone sufficient ancient heating for the TL-signal to be zeroed making it suitable for TL dating. The heating plateaus include the NTL peak and produced values in the order of about 345 - 400 °C (Fig. 3-5).

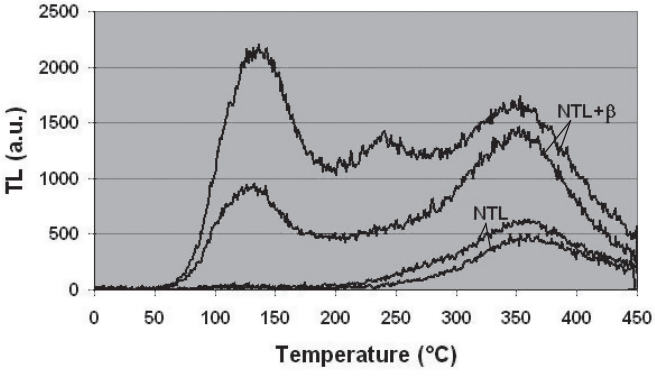


**Fig. 3-4** TL glow curve of test measurements.

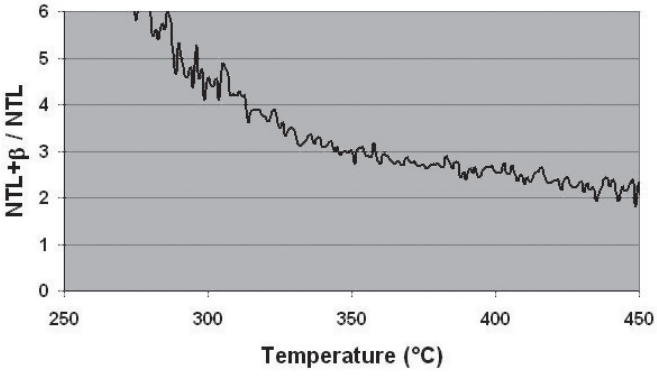


**Fig. 3-5** Heating plateau test (ratio NTL+β NTL) for the test analysis.

Part of the 90-160 μm fraction was heated in a furnace to 360°C for 90 min under air to provide thermally zeroed material for establishing a regenerated TL growth curve. Chemical preparation with 10% HCl and the use of a defloculant in the case of the coarse grains completed the sample preparation.

TL measurements were performed in a $N_2$ atmosphere in a Risø DA-15 system, with a bi-alkala photomultiplier tube, with the detection restricted to the UV-blue region by a Schott BG25 and a Hoya HA-30 filter. A heating rate of 5 °C $s^{-1}$ to 450 °C was employed with immediate background subtraction.

Samples were β-irradiated in the Risø DA-15 system with a calibrated $^{90}Sr/^{90}Y$-source (about 0.109 Gy $s^{-1}$), while α-irradiations were done in a Littlemore 721A under vacuum with six $^{241}Am$ sources, calibrated to about 0.187 $\mu m^{-2}$ $min^{-1}$. Irradiated samples were stored for 3-4 weeks at room temperature before being TL measured.

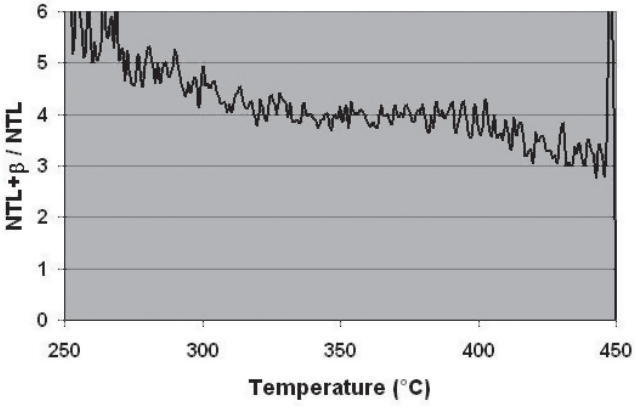


**Fig. 3-6** 2nd heating plateau test (ratio NTL+β NTL) for the interior of the flint sample.

## Second test for sufficiency of heating

Next the heating plateau test was repeated using material from the extracted core in order to verify that the interior of the sample had been sufficiently heated thus ensuring that the TL-signal was completely zeroed (Fig. 3-6). The heating plateau is similar to the one obtained from material from the edge of the sample and indicates the sufficiency of heating of the interior of the clast. The heating plateau of this second test fell in the range 335 - 400 °C (Fig. 3-6).

## Thermoluminescence methods and analysis

The potential age of the sample suggests that the NTL is well within the linear range of the additive TL growth curve. Four additive dose points were given and a regeneration growth curve with corresponding dose points was measured. The palaeodoses were calculated from the least square linear regression results from these two dose curves (Aitken 1985; Valladas 1992). The alpha sensitivity (b-value) was determined on material zeroed in the laboratory at 500°C for 30 min.

Data analysis was performed with the software Analyst. The integration range was defined as the joint temperature range of the heating (Fig. 3-7) as well as of the $D_e$-plateau (Fig. 3-8) for the additive dose curve. The latter is the temperature region of constant results of the equivalent dose ($D_e$) determination. The presence of such a plateau is another indication of the sufficiency of the prehistoric heating and that the samples are well zeroed.

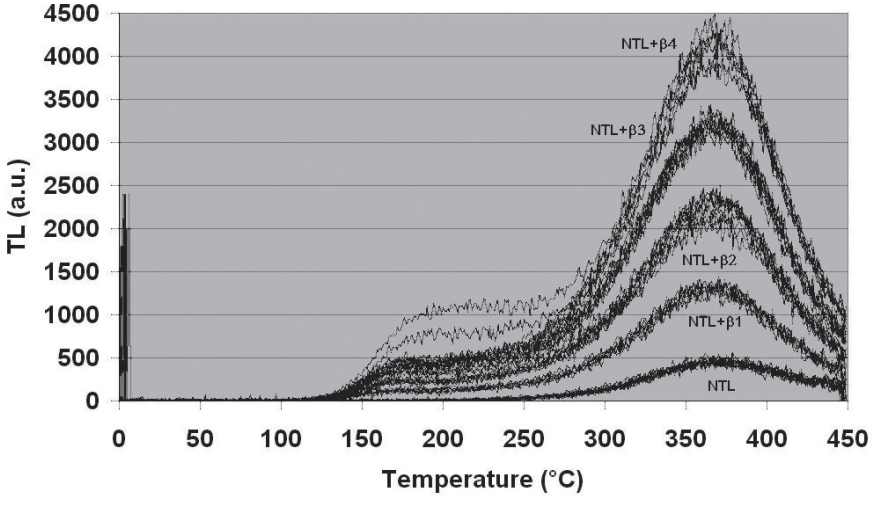


**Fig. 3-7** TL curves for sample EFD4L 264.

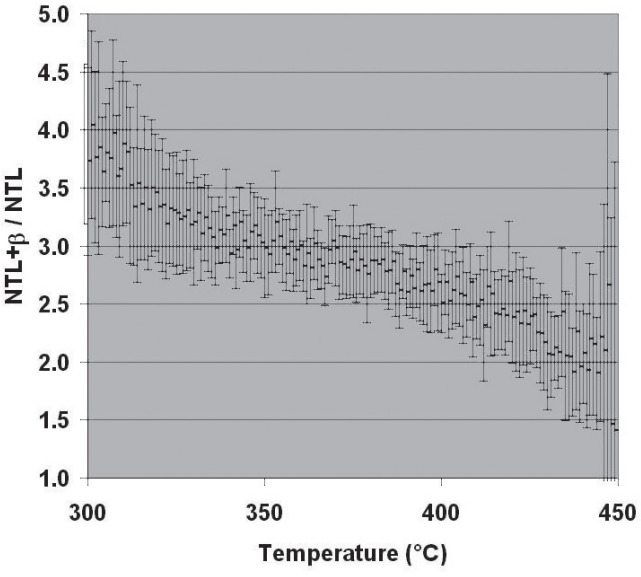


**Fig. 3-8** Heating plateaus for sample EFD4L 264 (340-390°C).

## Results

The TL additive and regeneration glow curves are shown in Fig. 3-7 with the resulting heating plateaus determined on the material/discs eventually used for palaeodose analysis (Fig. 3-8).

Unfortunately, the two growth curves for EFD4L 264 (Fig. 3-9) do not show a similar gradient of slope. This lack of supralinearity indicates that the sample is subject to sensitivity change due to heating in the laboratory and that the natural TL peak could not be regenerated. Instead, several other peaks occur at lower temperatures. The supralinearity correction is thus not valid in this instance and can not be used for estimating the palaeodose. The resulting age has therefore to be regarded as a minimum age.

The cosmic dose rates were calculated after (Barbouti and Rastin (1983) and Prescott and Stephan (1982) taking into account the elevation above sea level, longitude and latitude, as well as a sedimentary overburden of 4 m for Kabazi V of 2.25 g $cm^{-1}$ average density. The overburden was assumed to have been constant for the entire burial time and an error estimate of 5% is assumed for these cosmic dose rate values. The external γ-dose rate from the sediment was measured with a portable NaI-scintillator and average values for several readings are given in Table 3-8 as $\dot{D}_{\gamma-ext.}$. Gamma spectrometry laboratory measurements on the milled sediment from around the luminescence samples revealed no significant secular disequilibria for the U-decay chains. However, there could have been changes in the U-decay chain and hence alterations in the gamma dose rates which can not be detected by this method. For example, disequilibrium could have occurred several times early in the history of the sediment, but today the chains are back in equilibrium. In general, such events can not be accounted for, but in many cases γ-spectrometry provides indications of such problems, which then can be accounted for. Here it is assumed that possible disequilibria in the decay chains have a negligible effect on the dose rates, which are given in Table 3-8. However, in order to allow for any such variation or changes in the external γ-dose rate caused by changing water contents, an error estimate of 20% is used for age calculation.

The element concentration for U, Th and K were determined with INAA and ICP-MS on samples crushed to <50 μm. While the results for U and Th were identical with the two methods, the K content varied by several orders of magnitude. ICP-MS analysis were repeated several times, but failed to provide consistent results for K, emphasising the problems for measuring this isotope with that particular method. Neither ratio of these elements measured with INAA corresponds to the average ratios observed for the composition of the earth's crust either. However, it can be questioned if the crust ratio is necessarily valid for flint (a quick literature survey does not suggest any correlation). We prefer to use the results obtained by INAA in this study. Because of the small size of sample EFD4L264 the element concentrations were obtained with IC-MS on extracted (interior) material, while for INAA material which was cut off from the outer part of the sample had to be used. The values obtained by the latter might not represent the element concentration of the part used for luminescence analysis because of geochemical changes and/or zoning. However, U and Th results agree well between these two methods on those different parts of the sample, which seems to suggest that any differences for K are likely not significant.

The alpha sensitivity of the samples is extremely low, which leads to very small internal dose rates. The ages are thus heavily dependant on the estimation of the external gamma and cosmic dose rates. While for the latter an error of 5% is assumed, the associated error for the external gamma dose was set to 20% in order to include the effects of possible variations due to changes in water content or in the geometries used. The result is a value of 81±9 ka as a minimum age for sample EVA-LUM-06/02 (EFD4L264) due to the failure for supralinearity correction previously described (Table 3-9).

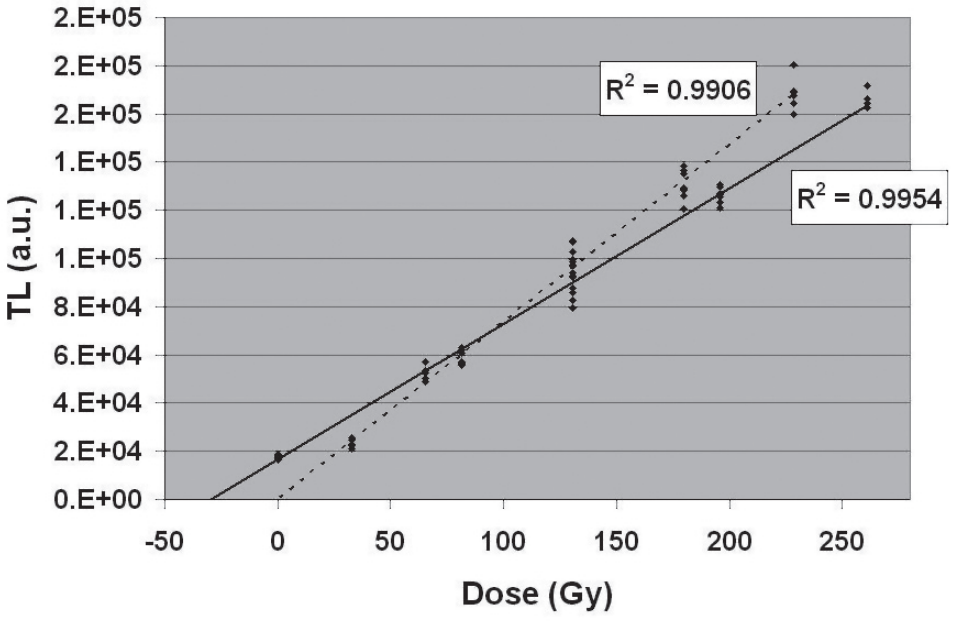


**Fig. 3-9** TL growth curves for sample EFD4L 264. The additive growth curve is marked on the swiped line and the regeneration on the dotted line. The x-axis intercepts of the linear regression give the $D_E$ for the additive growth curve and the supralinearity correction $D_I$ for the regeneration growth curve.

| Sample No.: | NTL peak (°C) | Heating plateau (°C) | $D_E$-plateau (°C) | b-value |
|---|---|---|---|---|
| EFD4L 264 | 370 | 340-390 | 350-400 | 8.0 ± 0.4 |

**Table 3-7** Summary of TL analysis results.

| Sample No. | U (ppm) | Th (ppm) | K (ppm) | $\dot{D}_{\alpha-\mathrm{int.}}$ (•Gy a$^{-1}$) | $\dot{D}_{\beta-\mathrm{int.}}$ (•Gy a$^{-1}$) | $\dot{D}_{\cos m.}$ (•Gy a$^{-1}$) | $\dot{D}_{\gamma-ext.}$ (•Gy a$^{-1}$) |
|---|---|---|---|---|---|---|---|
| EFD4L 264 | 0.13 ± 0.01 | 0.19 ± 0.12 | 485 ± 15 | 24 | 62 | 157 | 184 |

**Table 3-8** Summary of dosimetric results.

| EVA-LUM- | Sample No. | palaeodose (Gy) | $\dot{D}_{\mathrm{int.}}$ (•Gy a$^{-1}$) | $\dot{D}_{ext.}$ (•Gy a$^{-1}$) | age (ka) |
|---|---|---|---|---|---|
| 06/01 | EFD4L264 | 32.3 ± 1.0 | 101 | 399 | 81 ± 9 |

**Table 3-9** Summary of results and ages for sample EVA-LUM-06/01 (EFD4L 264) from Kabazi V.

# AMS Radiocarbon

## Methodology and results

One charcoal and one charred bone sample (EFD4C 420 & 436) were chemically pretreated in Oxford with the routine acid-alkali-acid (AAA) pre-treatment. This is designed to mobilise the two major contaminants present in soils that may affect radiocarbon dating of these types of samples, humic acids and fulvic acids. Both are organic compounds derived from the decayed remains of plants in the surface layers of the soil. Their presence in archaeological charcoals may constitute error of unknown magnitude and is highly site specific. Humic substances within the soil have been classified according to the ease with which they can be removed from soils using alkaline solutions (Head 1987). Humic acids may be defined as the fraction extracted by alkaline solution that becomes insoluble after acidification (Head 1987: 144). Fulvic acids are soluble both in acid and alkaline solutions (Head 1987). The residue soluble and insoluble in alkaline solutions is termed "humin" and is usually the fraction targeted for radiocarbon dating. In this instance the two dated fractions were not the "humin" residue, for in one case (the charred bone, EFD4C 420) the sample became soluble when treated with a solution of sodium hydroxide. In effect, this sample is the humic acid fraction and for this reason has been given an OxA-X designation to show that the age is less reliable than the chemically more rigorously treated samples. OxA-X-2134-45 is best seen as no more than a minimum age estimate for the horizon from which it came.

The four bone samples (EFD4C 419, 421, 435 & 437) were chemically pretreated using the standard Oxford method of the time, however all four produced very low percentage yields below 1% (Table 3-10). These values are considerably less than the threshold that Oxford considers to be needed to produce reliable age estimates and so no further analysis was undertaken. The results of dating for the two successful samples are shown in Table 3-10 – with OxA-14726 being considered the more reliable.

| Sample No. | | Lab No. | Treatment fraction | Sample wt. (mg) | Yield (mg) | %Yield | δ13C (per mil) | Age (uncal. years BP) |
|---|---|---|---|---|---|---|---|---|
| EFD4C | 419 | P16819 | - | 580.0 | 0.69 | 0.10 | - | - |
| EFD4C | 420 | OxA-X-2134-45 | Humic acids | 367.0 | 61.60 | 16.80 | -24.5 | 30,980 ± 220 (% mod 2.1 ± 0.1) |
| EFD4C | 421 | P16821 | - | 580.0 | 0.20 | 0.00 | - | - |
| EFD4C | 435 | P16822 | - | 550.0 | 1.80 | 0.30 | - | - |
| EFD4C | 436 | OxA-14726 | Humin | 137.7 | 35.60 | 25.90 | -22.8 | 38,780 ± 360 |
| EFD4C | 437 | P16824.0 | - | 520.0 | 0.46 | 0.10 | - | - |
| EFD4C | 437 | P16824.1 | - | 540.0 | 0.70 | 0.10 | - | - |

**Table 3-10** AMS $^{14}C$ age determinations from Kabazi V.

# Discussion

It is clear that the site of Kabazi V presents considerable challenges to the application of scientific dating methodologies. Rink et al. (1998, 339) gave a best age estimate for archaeological horizon III/1 of c. 26-30 ka BP, whilst the estimate for the stratigraphically lower level III/1A produced an age of <41 ka. In contrast, on the basis of four tooth enamel measurements McKinney (1998, 351) estimated that archaeological horizon III/1 at Kabazi V had an age of c. 73.3±6.0 ka.

The luminescence data from our studies in general supports the 'high chronology' for the site proposed by McKinney (1998) on the basis of U-series determinations, for the TL dating of sample EFD4L 264 indicates a minimum age of 81±9 ka, whilst the OSL profiling would indicate apparent ages down sequence of c. 60-100 ka. In contrast, the ESR favours a 'low chronology' of around 26-30 ka or <41 ka, placing the site chronologically within MIS 3.

An important problem arises when attempting to directly compare the pair of radiocarbon determinations produced in this study with the luminescence results, and the existing electron spin resonance and mass spectrometric U-series datasets of

Rink et al. (1998) and McKinney (1998), in that radiocarbon ages are not equivalent to absolute dates produced by other methodologies. At present it is not possible to reliably calibrate radiocarbon ages greater than 26 ka cal BP (Reimer et al. 2004) because there is no agreement on which of the various terrestrial and marine datasets that map the variation of $^{14}C$ production over time is likely to be the most accurate. In this study not having an agreed calibration dataset does not alter the broad conclusions, which is that the $^{14}C$ data better support the 'low chronology' hypothesis.

## Conclusions

Despite many attempts and varied methodologies the dating of Kabazi V remains unresolved. In this paper OSL profiling has been used to assess the prospects of dating the sediments in the matrix of the site. It appears that there is sufficient luminescence sensitivity in all phases examined for quantitative work to be undertaken. The apparent ages of the initial profiling work suggest that coarse grain sedimentary chronologies in the 60-100 ka or earlier range might be expected from the tube samples collected but not yet measured. This may include residual signals accumulated in upslope positions prior to colluvial re-deposition and it may be worth considering the possibility that single-grain coarse sediment dating could help to assess the extent to which such dates carry residual age.

The flint result obtained by MPI Leipzig gave extremely promising TL behaviour, with evidence from the "plateau curves" to verify that resetting by heat appears to have been achieved. The result from the sample dated is broadly consistent with the upper end of the implied sediment luminescence chronology, although again it is hard at this stage to know whether the item had been deposited in a primary context or had been incorporated by re-depositional process. Both luminescence methods indicate a significantly longer chronology than the carbon samples; although the difficulties associated with the latter measurements and their calibration have been noted and might be expected to lead to underestimated ages. It does appear therefore that further work on the sediment samples, possibly including single grain approaches, and further TL analyses on a larger assemblage of burnt flints may hold out the potential of getting a better chronology for the site. Together these approaches hold out the prospect of a profitable way forward in the future, for one positive outcome from this study has been the demonstration that the field gamma dosimetry of the site is remarkably consistent and stable. Because of this, heated clasts previously excavated could be used successfully for TL without too many difficulties, despite the loss of information arising from having removed the samples from their environment without recording the field dosimetry. Together these approaches hold out at least the potential for resolving a site that still is problematic in relation to the chronology of hominin occupation in the Middle Palaeolithic.

Abstract

# КАБАЗИ V: ЛЮМИНЕСЦЕНТНЫЙ АНАЛИЗ (OSL И TL) И РАДИОУГЛЕРОДНЫЕ (AMS) ОПРЕДЕЛЕНИЯ

*ХЁСЛИ Р. А., САНДЕРСОН Д. К. В., БАРБИДЖ К. И., РИХТЕР Д., ХИГАМ Т. Ф. Х.*

Для образцов из отложений Кабази V был получен ряд радиометрических определений. Фрагмент трубчатой кости из горизонта III/1A продатирован радиоуглеродным методом: OxA-X-2134-45, 30,98±0,22 тыс. лет назад. Образец древесного угля из горизонта III/5-3B2 получил радиоуглеродную дату OxA-14726, 38,78±0,36 тыс. лет назад. Достоверность результата полученного по образцу угля (OxA-14726) выше, чем достоверность даты полученной по образцу кости (OxA-X-2134-45). OSL параметры для литологических слоев 12 – 12A и 14A составляют 60-100 и 200 тысяч лет назад, соответственно. Минимальный TL возраст обожженного кремня из горизонта III/1A составил 81,0±9,0 тысяч лет назад.

Ранее по образцам эмалей зубов гидрунтинуса для горизонтов III/1 и III/1A была получена пара ESR показателей: 26–30 и <41 тысяч лет назад, соответственно (Rink *et al.*, 1998). Средний U-series возраст четырех образцов зубов гидрунтинуса из горизонта III/1 составил 73,3-0,6 (McKinney 1998)

Таким образом, хронологическое положение отложений Кабази V определяется двумя хронологическими шкалами – «короткой» и «длиной». «Короткой шкале» соответствуют даты, полученные радиоуглеродным и ESR методами. «Длинная шкала» образована TL, U-series и OSL показателями. На основании «короткой шкалы» можно сделать вывод о том, что отложения Кабази V аккумулировались во время OIS 3, тогда как «длинная шкала» относит образование стоянки к OIS 4 и OIS 5.